



Antimicrobial and anticancer activity of AgNPs coated with *Alphonsea sclerocarpa* extract

Suman Joshi D S Doddapaneni¹ · Chander Amgoth² · Arunasree M Kalle³ · Surya Narayana Suryadevara¹ · Krishna Satya Alapati¹

Received: 19 June 2017 / Accepted: 5 February 2018 / Published online: 2 March 2018
© Springer-Verlag GmbH Germany, part of Springer Nature 2018

Abstract

The synthesis and characterization of an aggregate of AgNPs coated with plant extract (PE) from *Alphonsea sclerocarpa* and its significant antimicrobial activity and inhibition on K562 (blood cancer) cells have been appended in the article. Synthesis of aggregate [(AgNPs)-(PE)] has been followed by a facile eco-friendly approach without using any harmful chemicals. The morphology of an aggregate [(AgNPs)-(PE)] was confirmed by TEM and SEM microscopic characterizations. Properties like solid state, the presence of functional groups, and elemental composition have been characterized through the XRD, FTIR, and EDAX. The biocompatibility of synthesized aggregate of [(AgNPs)-(PE)] was confirmed by the MTT assay. An in vitro cell (HEK293)-based studies were performed for the biocompatibility tests and it is found that the aggregate [(AgNPs)-(PE)] is not harmful to normal/healthy cells. Even though *A. sclerocarpa* show the antimicrobial (antibacterial and antifungal) activity, it has been further enhanced with the developed aggregate of [(AgNPs)-(PE)]. Furthermore, it has been extended to examine the cellular inhibition on K562 cells and obtained > 75% cell inhibition for 24 h treated cells.

Keywords [(AgNPs)-PE] · Silver nanoparticles · Antimicrobial activity · Cell inhibition

Introduction

Plants are the man's primary source of drugs for various diseases from the ancient times. Medicines derived from plants have played a pivotal role in health care of ancient and modern cultures (Petrovska 2012). Plants contain a plethora of compounds, including antioxidants, immune stimulants, cell proliferation stimulators, anti-inflammatory agents, anticancer components, and antimicrobial agents. A large number of plants with potential

therapeutic capabilities to cure a large number of ailments caused to man are identified and recognized globally. Plant-based materials have been demonstrated as excellent drug stores for therapeutic implants. However, Green tea, Cabbage, Holy basil leaves, Beets, *Aloe vera*, etc. are having potential and active functional groups which show antimicrobial activity and to cure several cancers. Likely, *Alphonsea sclerocarpa* is widely distributed in the state of Andhra Pradesh (India) and well known for its medicinal importance towards cancer therapy and antimicrobial usage. Every part of the *A. sclerocarpa* such as branches, bark, leaves, fruits, and flowers are extensively useful (Prasad 2009; Suman Joshi et al. 2017; Tacic et al. 1987). The plant extracts with the combination of metal nanoparticles such as silver (Ag), gold (Au), and iron oxide (FeO₃), Zinc (Zn), and cobalt (Co) show the enhanced properties towards the antimicrobial activity. Similarly, silver (Ag) and silver nanoparticles are well known for their oligodynamic property which means the capability to show biocidal activity even at low concentration (Siim et al. 2016). As per the literature, silver in its nanoscale size is exhibiting strong antimicrobial activity; it is further used as primary source for production of wide range

Electronic supplementary material The online version of this article (<https://doi.org/10.1007/s13205-018-1155-9>) contains supplementary material, which is available to authorized users.

✉ Krishna Satya Alapati
akrishnasatya78@gmail.com

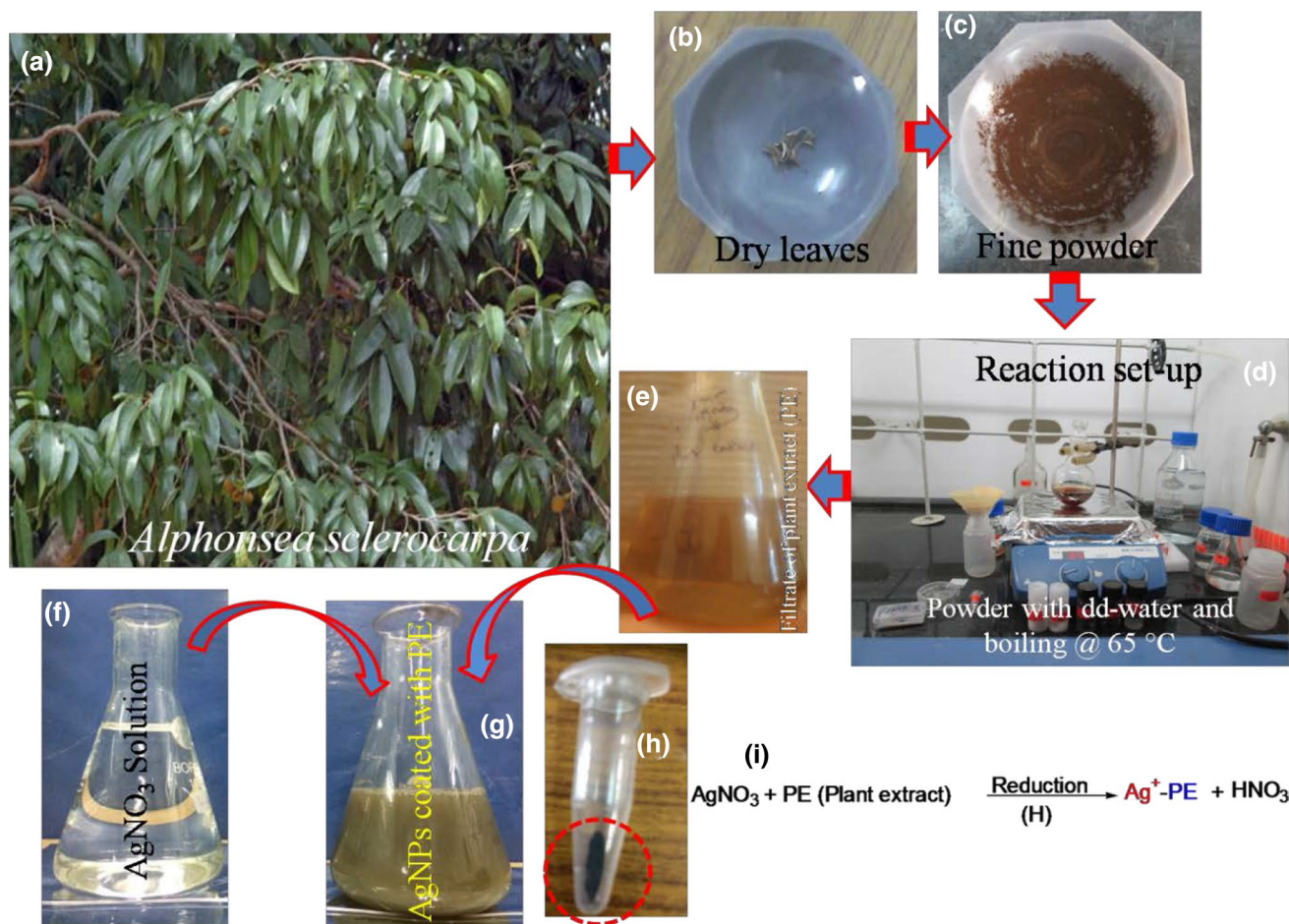
¹ Department of Biotechnology, Acharya Nagarjuna University, Nagarjuna Nagar, Guntur 522510, India

² School of Engineering Sciences and Technology, University of Hyderabad, Hyderabad, TS 500046, India

³ Department of Animal Sciences, School of Life sciences, University of Hyderabad, Hyderabad, TS 500046, India

of active functional materials. As per the global statistics, ~ 500 tons of silver nanoparticles were produced annually for the use of biomedical applications (Silver and Phung 1996; Morones et al. 2005; Mueller and Nowack 2008). Scientists and researchers are interested in curing diseases by the application of nanotechnology and nanobiotechnology through the development of plant-mediated metal nanoparticles (Irvani 2011). There are capsules, particles, and composite materials which have medicinal usages, but metal nanoparticles with the combination of plant extract are more efficient than their counterparts. After detailed literature survey on varieties of composite materials with the metal nanoparticles; we come across and decided to develop an aggregate with the help of silver nanoparticles and *A. sclerocarpa* extract. It is having a potential role towards antimicrobial and anticancer activity (Korbekandi et al. 2009; Irvani and Zolfaghari 2013).

Therefore, we focused on the extraction of phytochemicals from *A. sclerocarpa* and it is further used for the reduction of AgNO_3 to AgNPs through the in situ (single step) reduction reaction. The *A. sclerocarpa* extract has the affinity to interact with metal ions such as Ag^+ , Au^+ , Fe^+ , Zn^+ , etc. for the formation of composite materials and aggregates. The active functional groups which are present in the plant extract directly associated or interacted with the metal mentioned above ions and formed aggregates show significant and novel benefits towards for the usage of mankind. These are remarkable and effective reservoirs with antimicrobial activity and with sustained inhibition on various cancers (Morones et al. 2005). However, the effect of *A. sclerocarpa* alone shows the limited effect, but in combination with AgNPs, it shows enhanced and significant activity on bacterial and fungal species; it was chosen as a coating material for the AgNPs (El-Chaghaby and Ahmad 2011; Veerasamy et al. 2011) (Scheme 1).



Scheme 1 Steps involved in the synthesis of aggregate of AgNPs coated with *Alphonsea sclerocarpa* plant extract [(AgNPs)-(PE)]. Photo **a** for *Alphonsea sclerocarpa* leaves, **b** for dry leaves, **c** for grinded fine powder from leaves, **d** for reaction set-up, **e** plant extract,

f AgNO_3 solution, **g** for **e**, **f** of synthesized [(AgNPs)-(PE)] in the liquid form, **h** for [(AgNPs)-(PE)] in the powder form, and **i** for possible reduction reaction

Materials and methods

Collection of plant leaves

The leaves of plant *A. sclerocarpa* were collected from Seshachalam forest region of Andhra Pradesh, India identified with taxonomist, and a voucher specimen was deposited at Herbarium of Sri Venkateswara University with a voucher number 871. The leaves of the plant were collected, cleaned thrice with rinsing tap water to remove dirt, and allowed to dry at room temperature for a couple of weeks. The well-dried leaves were grinded into fine powder. The obtained fine powder was labelled and used for further experiments.

Synthesis of aggregate of [(AgNPs)-(PE)]

An amount of ~ 1.6 mg (0.0016 g) of silver nitrate (AgNO_3) was dissolved in ~ 250 mL of dd-water (H_2O) and stored as the stock solution for further use. Then, ~ 3.0 g of fine *A. sclerocarpa* powder was taken in a ~ 250 mL of round bottom (RB) flask and added with ~ 100 mL of dd- H_2O . The solution of AgNO_3 was added to RB flask and allowed to boil at ~ 65 °C for 1 h. However, boiling has been carried out with continuous stirring at 500 RPM on a magnetic hot plate. The colour of the mixture turned into light brown to dark brown after 1 h stirring at ~ 65 °C. After 1 h stirring, the mixture of *A. sclerocarpa* extract with AgNPs was filtered with Whatman filter paper, and it was recrystallized thrice. After a notable colour change upon incubation for 24 h, the [(AgNPs)-(PE)] was centrifuged at 8000 RPM for 20 min. The supernatant was discarded, and the pellet was collected and air dried.

Minimum inhibitory concentration (MIC)

The minimum inhibitory concentration (MIC) was defined as the minimum concentration required to inhibit the growth of the microorganisms by synthesized nanoparticles against both Gram-positive and Gram-negative bacteria, viz., *Bacillus subtilis*, *Lactobacillus acidophilus*, *Staphylococcus aureus*, *Streptococcus mutans*, *Escherichia coli*, *Pseudomonas aeruginosa*, *Klebsiella pneumonia*, and *Proteus vulgaris*. The MIC of AgNPs was determined using serial dilution microplate method (Eloff 1998; Andrews 2001). The bacterial inoculum was adjusted to match the tube of 0.5 McFarland turbidity standard using the spectrophotometer at 600 nm (Wavelength), which equals to ~ 1.5×10^8 colony-forming units (CFU)/mL (McFarland 1907). Different aliquots of AgNPs were mixed with the inoculums in test tubes and incubated at ~ 37 °C for 24 h. After incubation, MIC value of AgNPs against tested bacteria was calculated by taking the optical density of the

samples (Krishnan et al. 2015). All experiments were performed in triplicates and meant values along with standard deviation are represented. Nanoparticles dilution without inoculums was used as blank control, whereas Streptomycin was used as positive control and DMSO was used as negative control.

Antifungal activity

The antifungal activity was carried out using different fungal strains such as *Aspergillus brasiliensis*, *Aspergillus flavus*, *Aspergillus niger*, *Aspergillus solani*, and *Candida albicans*. Into the sterile Petri plates, 1 mL of the fungal suspension was taken followed by addition of molten state potato dextrose agar medium and mixed well. After complete solidification, wells were bored with sterile cork borer of 6 mm diameter followed by filling with ~ 100 μL of ~ 50 mg concentrated synthesized *A. sclerocarpa*-AgNPs which was dissolved in DMSO. The drug Fluconazole with the concentration of 10 $\mu\text{g}/100 \mu\text{L}$ was used as the standard antifungal agent (positive control). The Petri plates were incubated at ~ 25 °C for 72 h (Narayanan and Park 2014; Mallmann et al. 2015).

Cell inhibition assay (MTT assay)

The anticancer activity or inhibition capacity of a developed aggregate of [(*A. sclerocarpa*)-(AgNPs)] used to evaluate based on different cell lines. However, HEK293 (human embryonic kidney) are non-cancerous, and K562 (leukaemia blood) cancer cells were chosen for the cell inhibition assay (Amgoth et al. 2016). Well-cultured cell lines, ~ 4×10^5 cells/well were poured in the wells of 96-well plate in two series of sets with control and blank wells followed by the wells with [(AgNPs)-(PE)]. Then, wells containing ~ 4×10^5 cells/well were added with six different concentrations (1.0, 1.5, 2.0, 2.5, 3.0, and 3.5 $\mu\text{g}/\text{mL}$) of aggregate of developed [(AgNPs)-(PE)]. Furthermore, it was allowed to incubate for 24 h in a CO_2 incubator at ~ 37 °C. The purple formazan crystal formation was observed upon addition of MTT chemical which was dissolved in 100 μL dimethyl sulfoxide (DMSO). After 24 h incubation or treatment, 96-well plates were taken out from the incubator and used to analyze cell inhibition assay using BioTeck Synergy H⁴ model multiple readers (Jang et al. 2016). The obtained or recorded data have been collected from the instrument and used to plot a bar graph as represented in the results and discussion section (Fig. 5).

Results and discussion

Morphology of [(AgNPs)-(PE)]

The morphology of developed [(AgNPs)-(PE)] was characterized by the TEM (Transmission Electron Microscopy) imaging. From the TEM image studies, it is concluded that AgNPs are coated with *A. sclerocarpa* extract, and it appears as an aggregate of [(AgNPs)-(PE)]. The synthesized nanoscale AgNPs are confirmed through the TEM imaging and reported in Fig. 1. Figure 1 a, b corresponds to silver nanoparticles coated with *A. sclerocarpa* extract which shows the distribution of AgNPs and dispersion of *A. sclerocarpa* extract at lower magnification. The size of the AgNPs ranges from ~ 20 to 40 nm (in diameter) with an average size of 33 nm. The shape of the silver nanoparticles is irregular and inconsistent with a random distribution. The functional groups present in the phytochemicals (plant extract) are responsible for reduction and determination of AgNPs size and shape. The aggregate of AgNPs coated with *A. sclerocarpa* extract has shown in Fig. 1c, d at higher magnifications. It is clearly evidenced

that nanoscale silver particles have been coated with *A. sclerocarpa* extract. The yellow arrows in the image (c) (in Fig. 1) illustrate the distribution of metal (silver) nanoparticles bonded with PE. Since plant extract is sensitive at higher accelerating voltages (200 kV), samples for TEM imaging were added with phospho tungstic acid (PTA) to avoid the burning/charge affect at such high accelerating voltage (Protima et al. 2015). However, PTA forms a thin layer on the surface of the samples, and it resists/avoids the charge effect during imaging. Furthermore, the morphology of [(AgNPs)-(PE)] was confirmed by the SEM (Scanning Electron Microscopy) imaging. The SEM images in Fig. 2a–d corroborate the morphology of [(AgNPs)-(PE)]. From SEM, the clumsy aggregates of the plant extract with silver nanoparticles have been observed. Silver particles were surrounded by plant extract to form aggregates. Notably, silver nanoparticles are positively charged (Ag^+) and this could be the main reason for the formation of aggregates with plant extract. An aggregation between AgNPs and plant extract can be avoided with sonication methods based on our applications. The figure S1 c–d, (supporting information), shows the morphology of the aggregates of the [(AgNPs)-(PE)] at higher magnifications such as

Fig. 1 TEM images of an aggregate of AgNPs coated with *Alphonsea sclerocarpa* extract [(AgNPs)-(PE)]. Images from **a** to **d** are captured from lower to higher magnifications. Yellow arrows show the distribution of AgNPs coated with PE and dotted blue lines illustrate the dispersion of *Alphonsea sclerocarpa* extract

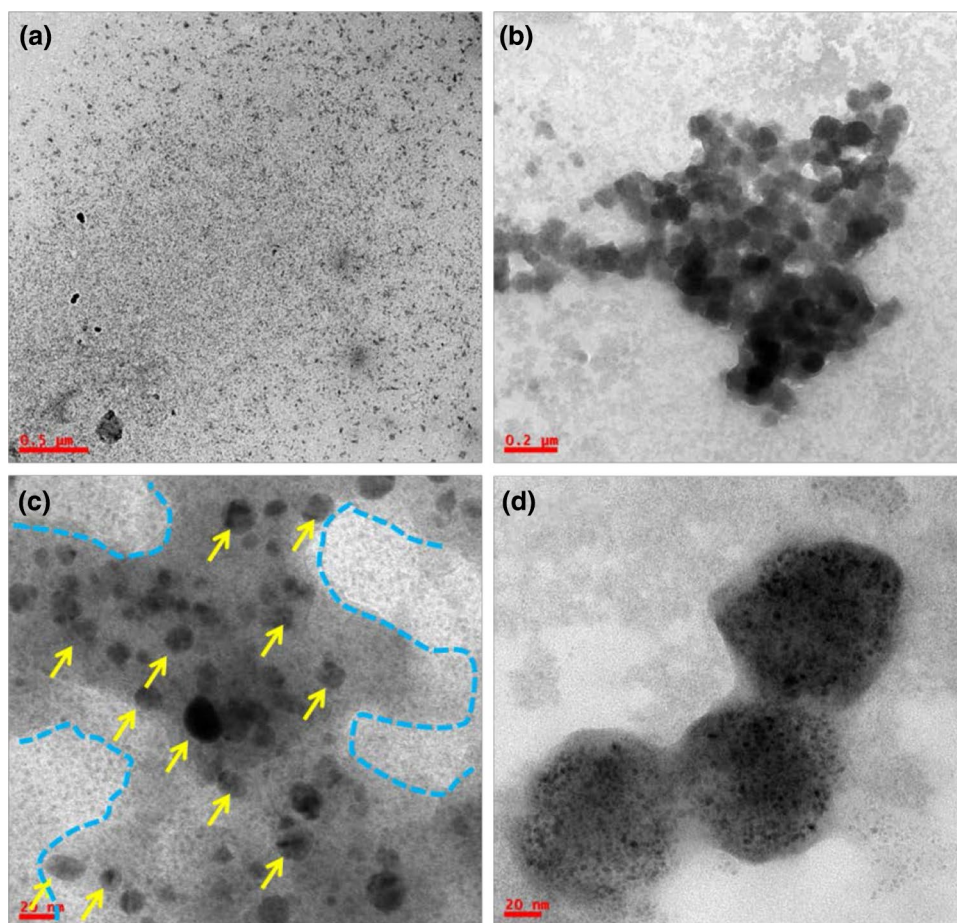
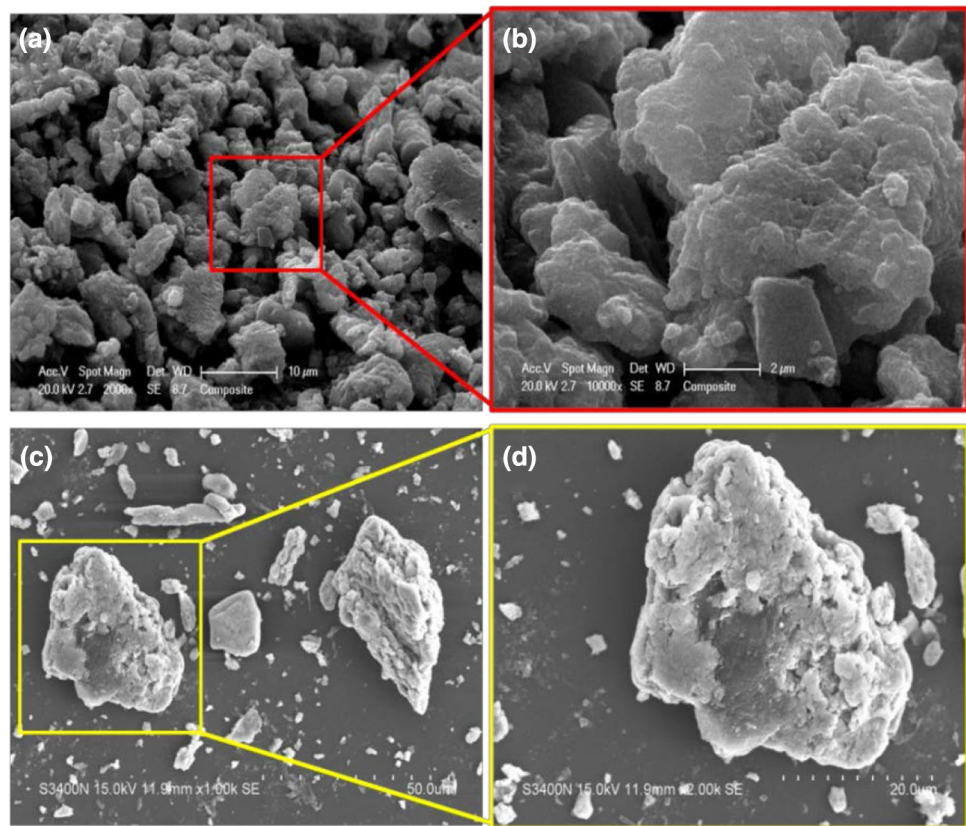


Fig. 2 SEM images of aggregate of AgNPs coated with *Alphonsea sclerocarpa* extract [(AgNPs)-(PE)]. Images **a, c** are acquired at lower magnification and **b, d** are acquired at higher magnification



500 nm. However, a non-conducting plant extract with AgNPs was sputter coated with conducting (Au) material to get the conductivity throughout the sample surface during SEM imaging (see supporting files). Furthermore, [(AgNPs)-(PE)] aggregate was characterized by FTIR (Fourier Transform Infrared), to know about the presence of functional groups. However, Fig. 3a illustrates the significant peaks for active functional groups. The peaks showed at $\sim 3304 \text{ cm}^{-1}$ (± 10) corresponds to the amide ($-\text{NH}$) group of the primary aromatic amine (Sastry et al. 1998), $\sim 2950 \text{ cm}^{-1}$ (± 10) corresponds to an asymmetric stretch of $-\text{CH}$ of the methyl group with SP^3 hybridization. The peak at $\sim 2428 \text{ cm}^{-1}$ (± 10) corresponds to an asymmetric stretch of $-\text{CH}$ and $\sim 1634 \text{ cm}^{-1}$ (± 10) peak corresponds to $-\text{NH}$ adjacent to methyl functional groups (Sastry et al. 1997; Biswajit Dey et al. 2013). The peak at ~ 1384 , 1246, and 1086 cm^{-1} corresponds to other functional groups present in the plant extract. Powder X-ray diffraction (XRD) has been performed to evaluate the solid state of developed [(AgNPs)-(PE)]-based aggregate and corresponding peaks for AgNPs were assigned in Fig. 3b. However, plant extract is amorphous in nature. It gives broad peak (noise) and crystalline nature of AgNPs was confirmed through the 2θ values on the x-axis; for example, $\sim 38^\circ$ for (111) planes, $\sim 45^\circ$ for (200) planes, $\sim 64^\circ$ for (220) planes, and $\sim 78^\circ$ for (311) planes. All together

correspond to the FCC (face-centered cubic) crystal structure of silver nanoparticles (Ma et al. 2001). The XRD peaks at 28 , 33 , 47 , 55 , 58 , and 82° (2θ) correspond to AgCl face-centered cubic structure. All the corresponding chlorine peaks were highlighted in the red circle in Fig. 3b, (Kumar et al. 2016). Furthermore, the synthesized [(AgNPs)-(PE)] has been used to analyze the elemental composition, and it has been achieved through the EDAX (Energy Dispersive X-ray Spectroscopy). The EDAX results in Fig. 4a, b shows weight and the atomic percentage of elements present in synthesized [(AgNPs)-(PE)] aggregate. The main peak is for source silver nanoparticles (AgNPs); C (Carbon) and O (Oxygen) are secondary source elements come from plant extract. However, the elements like Si (Silicon) and Au (Gold) are appeared in the sample because of contamination and as an impurity from sputter coating materials. The inset table in Fig. 4b shows the presence of all the elements in the developed aggregate of [(AgNPs)-(PE)]. From the EDAX, 57.23 weight (%) and 16.65 atomic (%) of Ag metal have been confirmed. The aggregated morphology of [(AgNPs)-(PE)] showed that, in TEM, images (Fig. 1) were evidenced/confirmed by the EDAX analysis. However, these silver nanoparticles were once again confirmed by using UV–visible spectrophotometric analysis (figure S2, Supporting information). The broad absorbance peak at $\sim 437 \text{ nm}$

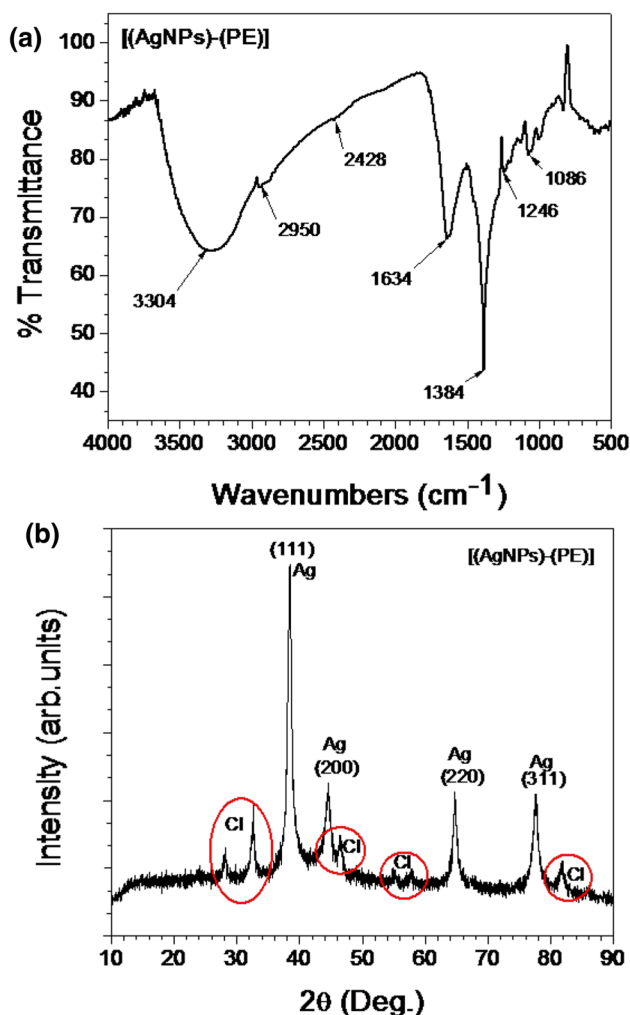


Fig. 3 Plot **a** corresponds to FTIR and **b** XRD for aggregate of AgNPs coated with *Alphonsea sclerocarpa* extract [(AgNPs)-(PE)]

corresponds to AgNPs. The appearance of the broad peak in AgNPs between ~ 400 and 500 nm is because of surface plasmon resonance (Sastry et al. 1998). The AgNPs from PE can be separated through the sonication methods. The optimization of sonication time and temperatures is key factors to consider separating the silver particles from PE.

Minimum inhibitory concentration (MIC)

The MIC values of *A. sclerocarpa*-AgNPs were given in Table 1 and the results revealed that the MIC values ranged from 8.66 ± 1.15 to 44.33 ± 0.57 mg/100 μ L against different bacteria tested. Lowest MIC value was observed against *Streptococcus mutans*, whereas higher MIC value was found to be against *Pseudomonas aeruginosa*. The difference between these MIC values among tested bacteria may be due to the structural difference between the cell wall of Gram-positive and Gram-negative bacteria. The reason

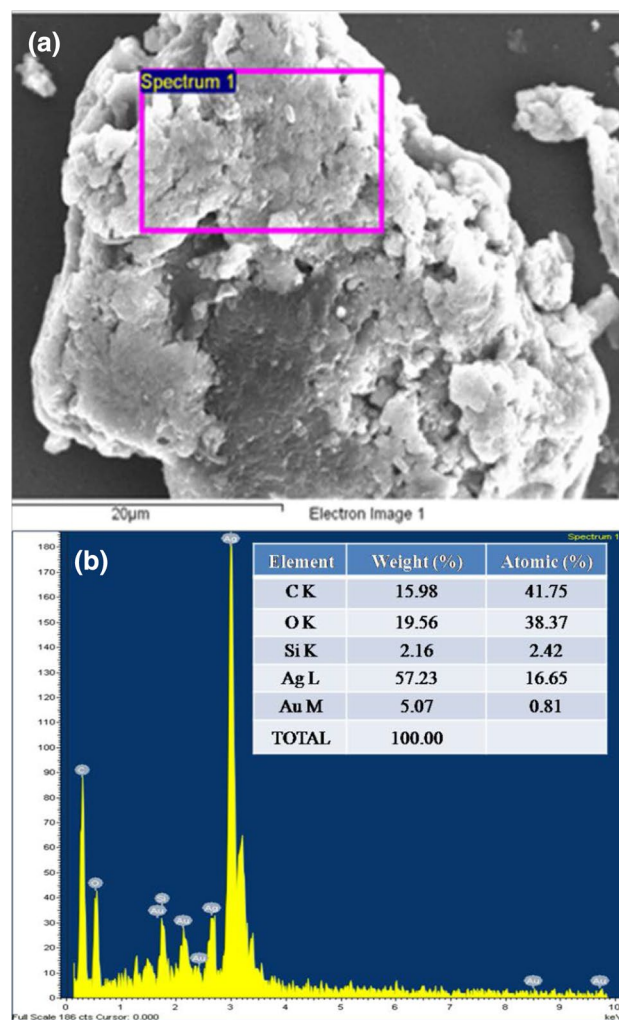


Fig. 4 EDAX images of aggregate of AgNPs coated with *Alphonsea sclerocarpa* extract [(AgNPs)-(PE)]. The inset table in the image **b** corroborates the presence of elements with their weight and atomic percentage

Table 1 Antibacterial activity on different bacteria species treated with an aggregate of AgNPs coated with *Alphonsea sclerocarpa* extract concerning minimum inhibitory concentration (MIC) (mg/100 μ L) values

S. no	Name of the organism	[(AgNPs)-(PE)] (MIC values)	Streptomycin (MIC values)
1	<i>Bacillus subtilis</i>	31.66 ± 1.15	7.00 ± 0.50
2	<i>Escherichia coli</i>	30.00 ± 1.73	1.66 ± 0.28
3	<i>Klebsiella pneumoniae</i>	20.00 ± 1.00	1.66 ± 0.28
4	<i>Lactobacillus acidophilus</i>	40.00 ± 1.00	2.33 ± 0.28
5	<i>Pseudomonas aeruginosa</i>	44.33 ± 0.57	2.33 ± 0.28
6	<i>Proteus vulgaris</i>	26.33 ± 1.50	6.00 ± 0.86
7	<i>Staphylococcus aureus</i>	14.66 ± 1.15	1.66 ± 0.28
8	<i>Streptococcus mutans</i>	8.66 ± 1.15	1.66 ± 0.28

for the antibacterial activity of AgNPs was reported earlier which may be due to the penetrating of silver ions into cells and intercalating between purine and pyrimidine bases leading to denaturation of DNA (Ahmed et al. 2016). It is also evident from earlier reports that the signal transduction in bacteria is regulated and determined by the phosphorylation of proteins. The AgNPs are reported to alter the peptide substrates leading to dephosphorylation of tyrosine residues in proteins, thus inhibiting the cell signalling and leads to cell death (Shrivastava et al. 2007; Nagababu and Uma Maheswara Rao 2017).

Antifungal activity

Similarly, to examine the antifungal activities, fungal inhibition with the developed [(AgNPs)-(PE)]-based aggregate has been evaluated using five different types of fungal species, as reported in Table 2. As per the results obtained, the high (19.5 ± 0.29) antifungal activity (fungal inhibition) with [(AgNPs)-(PE)] was observed on *Aspergillus brasiliensis* and least inhibition (10 ± 0.81) on *Aspergillus flavus*. The results compared with positive control are represented in Table 2 and Figure S3, (supporting information). However, AgNPs with plant extract show enhanced antifungal activity. It is attributed based on various factors such as particle size (typically particle size should be in the range of $\sim 20\text{--}50$ nm). The increase in specific surface area promotes better contact and interaction with bacterial and fungal species leading to reducing their further proliferation (Feng et al. 2000; Lok et al. 2006; Rai et al. 2009; Siim et al. 2016). However, penetrated AgNPs will induce free radicals and cause oxidative stress leading to inhibition of bacteria and fungi (Morones et al. 2005; Song et al. Song et al. 2006).

Cellular inhibition assay and imaging

From the obtained data, bar graph was plotted and it shows increased inhibition tendency as the increase of the concentration of aggregate of [(AgNPs)-(PE)]. The concentration of aggregate of [(AgNPs)-(PE)] with $1.0 \mu\text{g}$ (IC_{50}) shows

Table 2 Antifungal activity with the synthesized aggregate of [(AgNPs)-(PE)] and comparison with standard fluconazole

S. no	Name of the organism	[(AgNPs)-(PE)] zone of inhibition (mm)	Fluconazole zone of inhibition (mm)
1	<i>Aspergillus brasiliensis</i>	19.5 ± 0.29	$24. \pm 0.59$
2	<i>Aspergillus flavus</i>	$10. \pm 0.81$	14.3 ± 0.97
3	<i>Aspergillus niger</i>	10.7 ± 0.39	12.6 ± 0.43
4	<i>Aspergillus solani</i>	10.2 ± 0.70	12.9 ± 0.21
5	<i>Candida albicans</i>	11.7 ± 0.30	13.6 ± 0.65

greater than 50% cell inhibition and for $3.5 \mu\text{g}$. It is measured as greater than 75%, which is ever reported with such aggregate of [(AgNPs)-(PE)], (silver nanoparticles coated with *A. sclerocarpa* extract). Blank well is used as zero inhibition without any developed [(AgNPs)-(PE)] compounds. However, inhibition is observed on cancerous (K562) cells only; the inhibition on normal HEK293 cells is negligible which is less than 10%. With these results, it is evidenced as the synthesized aggregate of [(AgNPs)-(PE)] can be used to treat the cancer cells Fig. 5. The K562 cells used for cellular inhibition assay were once again added with different fluorescent dyes and used for morphological imaging. Figure 6a–d illustrates the morphology of K562 cells which are stained with FITC (green fluorescent dye) and Rhodamine-B (red fluorescent dye) which stains cytoplasm of cells and DAPI (blue fluorescent dye) which mainly stains genetic material of DNA/RNA. Specifically, it stains A-T, (adenine–thymine)-rich regions. Figure 6d depicts the merged images of cells with different fluorescent dyes. From these fluorescent images of K562 cells, it is confirmed that the cellular rupture and morphological distortions are occurred compared to optical microscopy images in figure S4, (Supporting information).

Conclusions

Herein, silver nanoparticles were successfully coated with *A. sclerocarpa* extract to develop an aggregate of [(AgNPs)-(PE)]. The *A. sclerocarpa* extract has been used as reducing agent as well as binding glue to silver

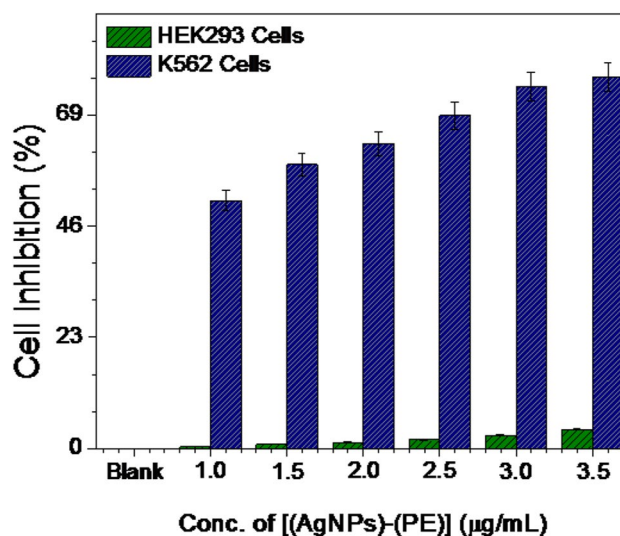
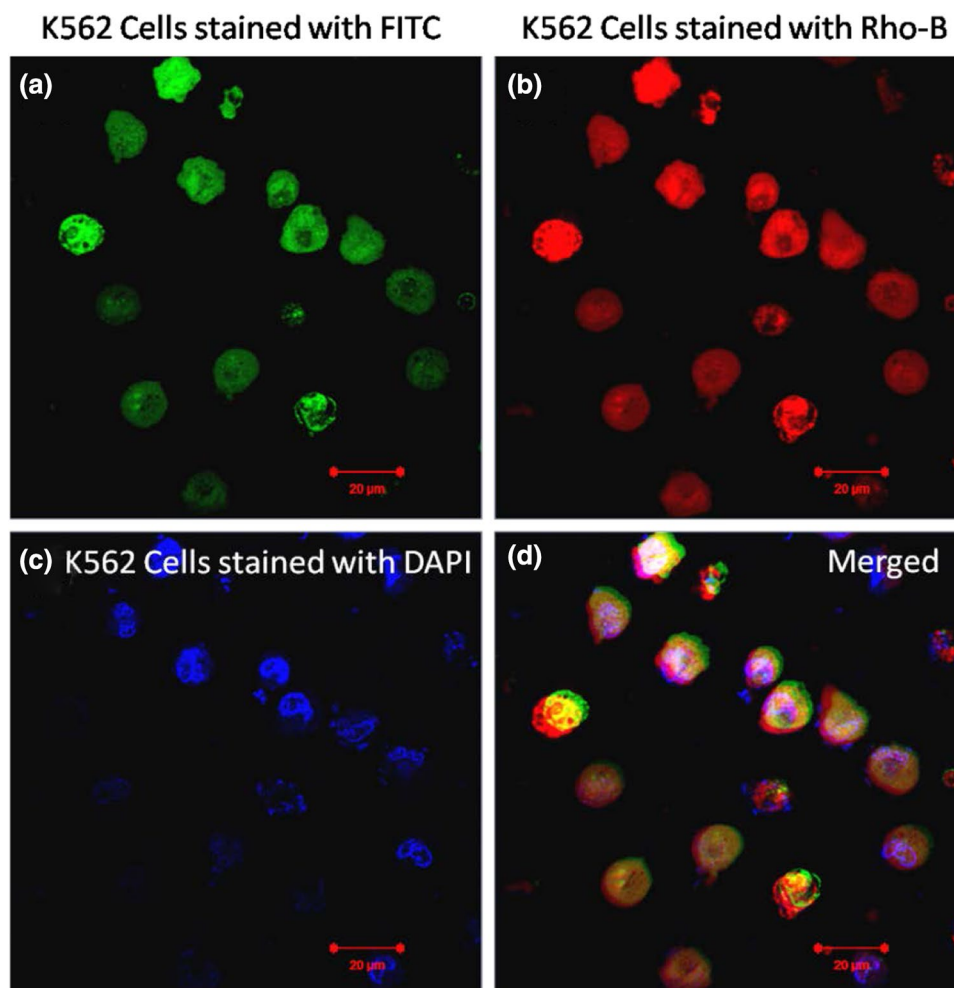


Fig. 5 Cell inhibition assay on cell lines. Inhibition with AgNPs coated with *Alphonseasclerocarpa* extract [(AgNPs)-(PE)]. Show more inhibition of cancerous K562 cells and inhibition is negligible on non-cancerous HEK293 cells

Fig. 6 Laser scanning confocal microscopic images of K562 cells acquired after 24 h treatment with AgNPs coated with *Alphonsea sclerocarpa* extract [(AgNPs)-(PE)]



nanoparticles. The developed [(AgNPs)-(PE)] was characterized using various microscopic techniques. [(AgNPs)-(PE)] is biocompatible for non-cancerous cells. It is a new approach to develop [(AgNPs)-(PE)] aggregate with enhanced antimicrobial and anticancer activities. It is a green synthesis followed by the facile eco-friendly approach. Through this atom economy reaction, we have developed [(AgNPs)-(PE)], and it shows enhanced anticancer activity upon 24 h treatment on leukaemia blood cancer (K562) cells. The cellular inhibition with [(AgNPs)-(PE)] is calculated as $> 75\%$, which is ever reported with such type of materials. Furthermore, the bacterial inhibition was found to be highest with *Pseudomonas aeruginosa* with 44.33 ± 0.57 mg/100 μ L, whereas for fungal species, highest inhibition is found for *Aspergillus brasiliensis* with an inhibition of 19.5 ± 0.29 . Furthermore, these types of aggregates can be recommended for other biomedical and pharmaceutical applications.

Acknowledgements The authors would like to acknowledge DST-FIST, Department of Physics, Acharya Nagarjuna University for

providing IR facility, University of Hyderabad, for providing SEM with EDAX and XRD facility.

Compliance with ethical standards

Conflict of interest Both the first and second authors have equal contribution to the paper.

References

- Ahmed S, Ahmad M, Swami BL, Ikram S (2016) A review on plants extract mediated synthesis of silver nanoparticles for antimicrobial applications: a green expertise. *J Adv Res* 7:17–28
- Amgoth C, Dharmapuri G, Kalle AM, Paik P (2016) Nanoporous capsules of block copolymers of [(MeO-PEG-NH)-b-(L-GluA)]-PCL for the controlled release of anticancer drugs for therapeutic applications. *Nanotechnology* 27(12):125101
- Andrews JM (2001) Determination of minimum inhibitory concentration. *J Antimicrob Chemother* 48(1):5–16
- Dey Biswajit, Saha Rajat, Mukherjee Priyanka (2013) A luminescent-water soluble inorganic co-crystal for a selective picomolar range arsenic (III) sensor in a water medium. *Chem Commun* 63:7064–7066

- El-Chaghaby GA, Ahmad AF (2011) Biosynthesis of silver nanoparticles using *Pistacia lentiscus* leaves extract and investigation of their antimicrobial effect. *Orient J Chem* 27(3):929–936
- Eloff JN (1998) A sensitive and quick microplate method to determine the minimal inhibitory concentration of plant extracts for bacteria. *Planta Med* 64:711–713. <https://doi.org/10.1055/s-2006-957563>
- Feng QL, Wu J, Chen GQ, Cui FZ, Kim TN, Kim JO (2000) A mechanistic study of the antibacterial effect of silver ions on *E. coli* and *Staphylococcus aureus*. *J Biomed Mater Res* 52(4):662–668
- Iravani S (2011) Green synthesis of metal nanoparticles using plants. *Green Chem* 13:2638–2650. <https://doi.org/10.1039/c1gc15386b>
- Iravani S, Zolfaghari B (2013) Green synthesis of silver nanoparticles using *Pinus eldarica* bark extract. *Biomed Res Int* 2013:639725. <https://doi.org/10.1155/2013/639725>
- Jang SJ, Yang IJ, Tettey CO, Kim KM, Shin HM (2016) In-vitro anticancer activity of green synthesised silver nanoparticles on MCF-7 human breast cancer cells. *Mater Sci Eng* 68:430–435. <https://doi.org/10.1016/j.msec.2016.03.101>
- Korbekandi H, Iravani S, Abbasi S (2009) Production of nanoparticles using organisms. *Crit Rev Biotechnol* 29:279–306. <https://doi.org/10.3109/07388550903062462>
- Krishnan R, Arumugam V, Vasaviah SK (2015) The MIC and MBC of silver nanoparticles against *Enterococcus faecalis*—a facultative anaerobe. *J Nanomed Nanotechnol* 6(3):285. <https://doi.org/10.4172/2157-7439.1000285>
- Kumar VA, Uchida T, Mizuki T, Nakajima Y, Katsube Y, Hanajiri T, Maekawa T (2016) Synthesis of nanoparticles composed of silver and silver chloride for a plasmonic photocatalyst using an extract from a weed *Solidago altissima* (goldenrod). *Adv Nat Sci* 7(1):015002
- Lok CN, Ho CM, Chen R, He QY, Yu WY, Sun H, Tam PK, Chiu JF, Che CM (2006) Proteomic analysis of the mode of antibacterial action of silver nanoparticles. *J Proteome Res* 5(4):916–924. <https://doi.org/10.1021/pr0504079>
- Ma CY, Rout MK, Mock WY (2001) Study of oat globulin conformation by Fourier transform infrared spectroscopy. *J Agric Food Chem* 49:3328–3334
- Mallmann EJ, Cunha FA, Castro BN, Maciel AM, Menezes EA, Fechine PB (2015) Antifungal activity of silver nanoparticles obtained by green synthesis. *Rev Inst Med Trop Sao Paulo* 57(2):165–177. <https://doi.org/10.1590/S0036-46652015000200011>
- McFarland J (1907) Nephelometer: an instrument for estimating the number of bacteria in suspensions used for calculating the opsonic index and for vaccines. *J Am Med Assoc* 14:1176–1178. <https://doi.org/10.1001/jama.1907.25320140022001f>
- Morones JR, Elechiguerra JL, Camacho A, Holt K, Kouri JB, Ramirez JT, Yacaman MJ (2005) The bacterial effect of silver nanoparticles. *Nanotechnology* 16(10):2346–2353. <https://doi.org/10.1088/0957-4484/16/10/059>
- Mueller NC, Nowack B (2008) Exposure modelling of engineered nanoparticles in the environment. *Environ Sci Technol* 42:4447–4453
- Nagababu P, Uma Maheswara Rao V (2017) Pharmacological assessment, green synthesis and characterization of silver nanoparticles of *sonneratia apetala* Buch.-Ham. leaves. *J App Pharm Sci* 7(8):175–182
- Narayanan KB, Park HH (2014) Antifungal activity of silver nanoparticles synthesised using turnip leaf extract (*Brassica rapa L.*) against wood rotting pathogens. *Eur J Plant Pathol* 140:185–192. <https://doi.org/10.1007/s10658-014-0399-4>
- Petrovska BB (2012) Historical review of medicinal plants' usage. *Pharmacogn Rev* 6(11):1–5. <https://doi.org/10.4103/0973-7847.95849>
- Prasad DN (2009) Antioxidant activity of *Alphonsea sclerocarpa* bark. *Res J Pharmacol Pharmacodynamics* 1(2):66–69
- Protima R, Siim K, Stanislav F, Erwan R (2015) A review on the green synthesis of silver nanoparticles and their morphologies studied via TEM. *Adv Mat Sci Eng*. <https://doi.org/10.1155/2015/682749>
- Rai M, Yadav A, Gade A (2009) Silver nanoparticles as a new generation of antimicrobials. *Biotechnol Adv* 27(1):76–83. <https://doi.org/10.1016/j.biotechadv.2008.09.002>
- Sastry M, Mayya KS, Bandyopadhyay K (1997) pH-dependent changes in the optical properties of carboxylic acid derivatised silver colloidal particles. *Colloids Surf A* 127(1–3):221–228. [https://doi.org/10.1016/S0927-7757\(97\)00087-3](https://doi.org/10.1016/S0927-7757(97)00087-3)
- Sastry M, Patil V, Sainkar SR (1998) Electrostatically controlled diffusion of carboxylic acid derivatised silver colloidal particles in thermally evaporated fatty amine films. *J Phy Chem B* 102(8):1404–1410
- Shrivastava S, Bera T, Roy A, Singh G, Rama Chandra Rao P, Dash D (2007) Characterization of enhanced antibacterial effects of novel silver nanoparticles. *Nanotechnology* 18:1–9
- Siim K, Sander K, Protima R, Mithu G, David W, Erwan R (2016) Biocidal properties study of silver nanoparticles used for application in green housing. *Int Nano Lett* 6(3):191–197. <https://doi.org/10.1007/s40089-016-0186-7>
- Silver S, Phung LT (1996) Bacterial heavy metal resistance: new surprises. *Annu Rev Microbiol* 50:753–789
- Song HY, Ko KK, Oh IH, Lee BT (2006) Fabrication of silver nanoparticles and their antimicrobial mechanisms. *Eur Cell Mater* 11(1):58
- Suman Joshi DSD, Venkata Rao G, Satya Prasad M, Kishore Babu M, Surya Narayana S, Krishna Satya A (2017) Phytochemical screening and evaluation of antioxidant, antibacterial and antifungal activity of medicinal plant *Alphonsea sclerocarpa* Thaw. *J Pharmacogn Phytochem* 6(4):1280–1286
- Tacic D, Wannigama GP, Cassels BK, Cave A (1987) Alkaloids of *Alphonsea sclerocarpa*. *J Nat Prod* 50(3):518–519. <https://doi.org/10.1021/np50051a036>
- Veerasingam R, Xin TZ, Gunasagaran S, Xiang TFW, Yang EFC, Jeyakumar N, Dhanaraj SA (2011) Biosynthesis of silver nanoparticles using mangosteen leaf extract and evaluation of their antimicrobial activities. *J Saudi Chem Soc* 15:113–120. <https://doi.org/10.1016/j.jscs.2010.06.004>